J. Phys. Chem. Solids Vol. 39, pp. 1287–1294

0022-3697/78/1201-1287/$02.00/0

REPULSION PARAMETERS OF IONS AND RADICALS—APPLICATION TO PEROVSKITE STRUCTURES

RAMESH NARAYAN and S. RAMASESHAN
Materials Science Division, National Aeronautical Laboratory, Bangalore 560017, India

(*Received* 6 *January* 1978; *accepted in revised form* 31 *May* 1978)

Abstract—The compressible ion approach to repulsion which has been shown to work well for the alkali halides (*J. Phys. Chem. Solids* **37**, 395 (1976); *Curr. Sci.* **46**, 359 (1977)) has been extended to other cubic ionic crystals. Repulsion parameters have been refined for a number of ions and radicals viz., Cu^+, Ag^+, Tl^+, Mg^{2+}, Ca^{2+}, Sr^{2+}, Ba^{2+}, Zn^{2+}, Cd^{2+}, Hg^{2+}, Mn^{2+}, Fe^{2+}, Co^{2+}, Ni^{2+}, Sm^{2+}, Eu^{2+}, Yb^{2+}, Pb^{2+}, H^-, O^{2-}, S^{2-}, Se^{2-}, Te^{2-}, NH_4^+, SH^-, SeH^-, BrO_3^-, ClO_3^-, ClO_4^-, CN^-, NH_2^-, NO_3^-, BH_4^-, BF_4^-, SO_4^{2-}, NH^{2-}. Using these parameters, calculations have been made on the lattice spacings and compressibilities of a number of perovskite-like crystals of the form $A^+B^{2+}C_3^-$. The predicted values agree well with experiment. In the case of four crystals viz., $LiBaF_3$, $LiBaH_3$, $LiEuH_3$ and $LiSrH_3$, there were large discrepancies between the calculated and observed lattice spacings. When these crystals were assumed to be of the *inverse* perovskite structure, calculations showed good agreement with the experimental data.

1. INTRODUCTION

The cohesive energy and static properties of ionic crystals have been of much interest to investigators during the last few decades. The attractive interactions in these crystals (viz. the electrostatic and dispersion forces) are quite well understood so that much of the effort has been directed towards computing the repulsive interaction (Ref. [1] gives a review of the field).

Recently, the authors proposed a new approach to the repulsion in ionic crystals based on a picture of compressible ions[2–4]. An ion is considered to be a soft sphere with an internal energy which is a function of its size. This leads to the hypothesis that the repulsion between ions arises entirely from the increase in their internal energies when compressed. It is also assumed that the energy of compression of an ion is local to its points of contact with neighbouring ions, so that, for a given radius, the internal energy of the ion is proportional to the number of its neighbours. By explicitly postulating an exponential form viz., $Ae^{-r/\rho}$, for the compression energy of individual ions, the repulsion parameters A and ρ have been calculated for all the ions in the alkali halides[5]. These parameters have been successful in describing many of the static properties of these crystals.

A theoretical justification has not yet been given for the basic postulates outlined above. However, there are some features in the present approach which are of *practical* importance. The repulsion parameters refined for an ion using the experimental data on any one crystal can be used unaltered in any other crystal of *any* structure in which the same ion occurs. This is in marked contrast to most earlier approaches to repulsion[1] in which some of the parameters can only be refined with experimental data on the very crystal in which one is interested.

The predictive power of the present theory is, however, an assertion which still needs to be tested. It has, in a sense, gained some credibility since the parameters of the alkali and the halogen ions could be used in the alkali halides of both NaCl and high pressure CsCl structures. In this paper we present a more comprehensive test of the predictive power of the theory. After a careful search, the perovskite class of crystals was chosen for this purpose. We present here calculations on the lattice spacings and the compressibilities of a number of perovskite-like crystals of the form $A^+B^{2+}C_3^-$ using repulsion parameters which were refined in *other simpler systems.*

The perovskite structure is relatively complex with three different types of ions per unit cell and with contacts occuring between a variety of pairs of ions. The repulsion parameters of the ions, on the other hand, were derived from the data on simple binary crystals of the NaCl, CsCl, ZnS, CaF_2 structures. Moreover, the regime of compression of the individual ions in these original crystals is often very different from that in the crystals studied in this paper. Consequently, the present calculations appear to be a critical test of our theory, as also of its usefulness in crystal physics.

As a preliminary to the studies on the perovskite-like crystals, repulsion parameters had to be refined for a variety of monovalent and divalent ions using experimental data on various binary crystals. The results of these studies are presented in Section 2. During this phase of the calculations, it was found that ionic *radicals* can also be treated within the framework of the present theory and this is discussed in Section 3. Section 4 details the theory of the various lattice interactions in the perovskite structure, in particular the repulsion energy as given by the present approach, while Section 5 deals with the evaluation of the attractive interactions. In Section 6 are presented the *predicted* lattice spacings and compressibilities of 31 perovskite-type crystals of the form $A^+B^{2+}C_3^-$. In the case of four crystals alone, there are large deviations from the experimental values. In Section 7 it is shown that these discrepancies can be reconciled if these crystals are assumed to be of the

inverse perovskite form. The Appendix deals with certain minor thermodynamic approximations that are necessary to carry out the calculations.

2. REPULSION PARAMETERS FOR MONOVALENT AND DIVALENT IONS

The equations that were developed for the calculations on the alkali halides[3] can with very slight modifications be applied to the crystals of interest here. The refinement procedures used in the present studies are just more sophisticated versions of the methods outlined in [3]. These details are therefore not discussed here.

For obtaining the repulsion parameters of Ag^+, Cu^+ and Tl^+, the experimental data (viz. the nearest neighbour distance and the bulk modulus) on their halides were used. Similarly, the repulsion parameters of H^- were refined using the data on the alkali hydrides. The repulsion parameters refined earlier[5] for the halogen and alkali ions were directly used unaltered and the parameters of only the new ions were refined. The optimised repulsion parameters are listed in Table 1 along with the values used for the alkali and halogen ions (included here for completeness).

A vast body of experimental data exists on crystals containing divalent ions. Using this, the repulsion parameters of the following divalent ions were refined—Mg^{2+}, Ca^{2+}, Sr^{2+}, Ba^{2+}, Zn^{2+}, Cd^{2+}, Hg^{2+}, Mn^{2+}, Fe^{2+}, Co^{2+}, Ni^{2+}, Sm^{2+}, Eu^{2+}, Yb^{2+}, Pb^{2+}, O^{2-}, S^{2-}, Se^{2-}, Te^{2-}. The values are listed in Table 1.

It should be mentioned that the repulsion parameters of Ag^+ and Hg^{2+} are not likely to be reliable because the fit between the calculated and observed quantities is quite unsatisfactory for the crystals containing these ions. Also, the parameters quoted for Zn^{2+}, Cd^{2+} and Hg^{2+} may not be meaningful since they have been refined on an ionic model using the experimental data on compounds such as ZnS which are generally believed to be quite covalent.

3. REPULSION PARAMETERS FOR IONIC RADICALS

At this point it appeared interesting to see whether the present theory of repulsion could be extended to ionic radicals. The fundamental postulate of our theory is that an ion has an internal compression energy which is a function of its size. In the case of ionic radicals, there are two contributions to the compression energy; (a) the compression of the closed shells of electrons of the outermost atoms, similar to the compression energy of simple ions, and (b) the energy arising from the compression of the covalent bonds in the radical. It may still be possible to express the overall compression energy of the radical as a simple monotonic function of its size.

To test whether this is so, we chose as our first example the ammonium radical. Good high pressure data are available on NH_4Cl, NH_4Br and NH_4I[6, 7]. We choose the same model function, viz. $Ae^{-r/\rho}$, that was used for all the ions studied earlier. The refined parameters of NH_4^+ are shown in Table 2. The fit with the experimental data is very good—the r.m.s. errors in r and d^2W_L/dr^2 are only 0.522% and 7.31% respectively. The fit is surprisingly even better than that obtained in the alkali halides[5] indicating that the soft sphere approach works well for ionic radicals.

Table 1. Repulsion parameters for monovalent and divalent ions

Ion	A (erg)	ρ(Å)	Ion	A(erg)	ρ(Å)
Li^+	0.1544×10^{-5}	0.04158	Co^{++}	0.9939×10^{11}	0.01737
Na^+	0.1211×10^{-7}	0.09029	Ni^{++}	0.1251×10^{12}	0.01656
K^+	0.5600×10^{-7}	0.1078	Sm^{++}	0.3309×10^{3}	0.04081
Rb^+	0.3980×10^{-5}	0.08883	Eu^{++}	0.3412×10^{6}	0.03370
Cs^+	0.5604×10^{-5}	0.09977	Yb^{++}	0.1104×10^{8}	0.02944
Cu^+	0.1222×10^{13}	0.01542	Pb^{++}	0.2814×10^{-4}	0.08017
Ag^+	0.3404×10^{-3}	0.05481			
Tl^+	0.7386×10^{-6}	0.1001			
			F^-	0.7506×10^{-10}	0.2152
Mg^{++}	0.9939×10	0.03051	Cl^-	0.2958×10^{-9}	0.2240
Ca^{++}	0.1471×10^{-4}	0.07017	Br^-	0.3724×10^{-9}	0.2352
Sr^{++}	0.3483×10^{-4}	0.07441	I^-	0.4407×10^{-9}	0.2538
Ba^{++}	0.1997×10^{-5}	0.09919	H^-	0.1604×10^{-10}	0.3150
Zn^{++}	0.1562×10^{-2}	0.04713			
Cd^{++}	0.3410×10^{-5}	0.07645	O^{--}	0.5135×10^{-10}	0.3160
Hg^{++}	0.6079×10^{23}	0.01680	S^{--}	0.3343×10^{-10}	0.3431
Mn^{++}	0.2941×10^{13}	0.01733	Se^{--}	0.6948×10^{-10}	0.3877
Fe^{++}	0.7895×10^{15}	0.01515	Te^{--}	0.1071×10^{-9}	0.3770

Table 2. Repulsion parameters for ionic radicals

Ion	A(erg)	ρ(Å)
NH_4^+	0.1688×10^{-4}	0.07820
SH^-	0.1759×10^{-7}	0.1545
SeH^-	0.1463×10^{-5}	0.1190
BrO_3^-	0.5821×10^{-5}	0.1200
ClO_3^-	0.4614×10^{-5}	0.1186
ClO_4^-	0.3489×10^{-9}	0.2724
CN^-	0.3460×10^{-9}	0.2288
NH_2^-	0.9310×10^{-7}	0.1149
NO_3^-	0.5882×10^{-9}	0.2354
BH_4^-	0.1294×10^{-9}	0.2682
BF_4^-	0.2959×10^{-4}	0.1068
SO_4^{--}	0.7213×10^{-9}	0.2838
NH^{--}	0.3258×10^{-10}	0.3954

Encouraged by this, the repulsion parameters of a number of other ionic radicals were determined. The refined parameters are listed in Table 2. Unfortunately, compressibility data seem to be available for only a few crystals containing these radicals viz., KCN, $Pb(NO_3)_2$[8], $NaClO_3$ and $NaBrO_3$[7]. Hence, the parameters of the radicals other than NH_4^+, ClO_3^-, BrO_3^-, NO_3^- and CN^- are not likely to be reliable.

Many of the ionic radicals studied, such as NO_3^-, are by no means spherical. The present model of spherical, compressible ions is, therefore, not likely to be valid for them. However, the reasonably good fit between theory and experiment raises questions as to why the approach works.

4. THEORY FOR PEROVSKITE-TYPE LATTICES

We shall now use the repulsion parameters available to compute the lattice spacings and compressibilities of some perovskite-like compounds. Figure 1 shows a unit cell of the cubic perovskite (ABC_3) structure. The A ions are at the cube corners, the B ions at the body centres and the C ions at the face centres. We require a knowledge of the number of contacts that each ion makes with its neighbours and also the distances of these neighbours. Using the symbol a for the cubic cell parameter,

(i) there is one A ion per molecule, having $12C$ neighbours, $8B$ neighbours and $6A$ neighbours at distances of $a/\sqrt{2}$, $\sqrt{3}a/2$ and a respectively,

(ii) there is one B ion per molecule, having $6C$ neighbours and $8A$ neighbours at distances of $a/2$ and $\sqrt{3}a/2$ respectively, and

(iii) there are $3C$ ions per molecule, each having $2B$ neighbours, $4A$ neighbours, $8C$ neighbours and a further $4C$ neighbours at distances of $a/2$, $a/\sqrt{2}$, $a/\sqrt{2}$ and a respectively.

In the present theory of repulsion, there are terms of the form $Ae^{-r/\rho}$ for each ion for every neighbour with which it makes contact, where A and ρ are the repulsion parameters associated with the ion and r is its radius in the direction of the neighbour of interest.

We use the following notation. We call the "radius" of an A ion in the direction of a neighbouring B ion as r_{AB}. Similarly, we define r_{AA}, r_{AC}, r_{BA}, r_{BB}, r_{BC}, r_{CA} and r_{CB}.

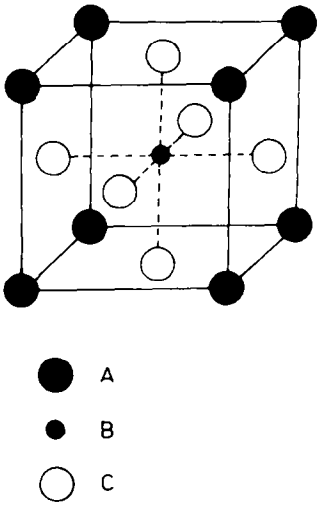

Fig. 1. Cubic unit cell of the Perovskite structure. In crystals of interest to the present paper, A is a monovalent cation, B is a divalent cation and C is a monovalent anion.

In the case of a C ion, since there are two types of C neighbours, r_{CC1} is its "radius" in the direction of the $8C$ neighbours at a distance of $a/\sqrt{2}$ and r_{CC2} is its "radius" in the direction of the $4C$ neighbours at a distance of a.

Using the structural information summarized above, we can now write the lattice energy per molecule as

$$\begin{aligned} W_L(a) = &-\frac{\alpha e^2}{a} - \frac{C}{a^6} - \frac{D}{a^8} + 6A_A e^{-r_{AA}/\rho_A} + 8A_A e^{-r_{AB}/\rho_A} \\ &+ 12A_A e^{-r_{AC}/\rho_A} + 8A_B e^{-r_{BA}/\rho_B} + 6A_B e^{-r_{BC}/\rho_B} \\ &+ 12A_C e^{-r_{CA}/\rho_C} + 6A_C e^{-r_{CB}/\rho_C} \\ &+ 24A_C e^{-r_{CC1}/\rho_C} + 12A_C e^{-r_{CC2}/\rho_C}. \end{aligned} \quad (1)$$

Here, α is the Madelung constant and C and D are the van der Waals dipole–dipole and dipole-quadrupole interaction coefficients (Section 5 discusses the calculation of these quantities). A_A and ρ_A are the repulsion parameters of the A ion, etc. In writing down the repulsion part of the interaction in (1), we have included a compression energy term for every contact an ion makes with its neighbours. As this is a straightforward extension of the basic ideas on which the present theory is built[3], we will not discuss it in detail here.

The energy W_L in (1) is a function of 10 variables viz., a, r_{AA}, r_{AB}, r_{AC}, r_{BA}, r_{BC}, r_{CA}, r_{CB}, r_{CC1}, r_{CC2}. We now identify a number of auxiliary conditions which relate the various "radii" among themselves and to the lattice spacing a. W_L will finally depend on only one variable viz., a.

The sum of the radii of two ions in contact is equal to their distance of separation. When the two ions are of different kinds, we obtain three relations of the type

$$r_{AB} + r_{BA} = \sqrt{3}a/2. \quad (2)$$

When the two ions are of the same kind, symmetry requires that the "radius" of each be half their separation, leading to three more relations of the type

$$r_{AA} = a/2. \quad (3)$$

Finally, we must use relations describing the condition for the internal equilibrium of the crystal at the points of contact of non-identical ions. Considering the AB contact, we have

$$\frac{\partial W_L}{\partial r_{AB}} = \frac{\partial W_L}{\partial r_{BA}} \tag{4}$$

which leads to

$$\frac{r_{BA}}{\rho_B} - \frac{r_{AB}}{\rho_A} = \ln \frac{A_B \rho_A}{A_A \rho_B}. \tag{5}$$

There are similar equations for the BC and AC contacts.

We thus have nine auxiliary conditions, as a result of which W_L is implicitly a function of only one variable, which we take to be a. We are therefore justified in talking of the total derivatives $dW_L(a)/da$ and $d^2W_L(a)/da^2$.

Differentiating (1) with respect to a and using the various expressions above, we get

$$\frac{d}{da} W_L(a) = \frac{\alpha e^2}{a^2} + \frac{6C}{a^7} + \frac{8D}{a^9} - \frac{3A_A}{\rho_A} e^{-a/2\rho_A} - \frac{6\sqrt{2}A_C}{\rho_C} e^{-a/2\sqrt{2}\rho_C} - \frac{6A_C}{\rho_C} e^{-a/2\rho_C} - \frac{4\sqrt{3}A_A}{\rho_A} e^{-r_{AB}/\rho_A} - \frac{6\sqrt{2}A_A}{\rho_A} e^{-r_{AC}/\rho_A} - \frac{3A_B}{\rho_B} e^{-r_{BC}/\rho_B}. \tag{6}$$

Differentiating (6) once more with respect to a, we obtain

$$\frac{d^2}{da^2} W_L(a) = -\frac{2\alpha e^2}{a^3} - \frac{42C}{a^8} - \frac{72D}{a^{10}} + \frac{3A_A}{2\rho_A^2} e^{-a/2\rho_A} + \frac{3A_C}{\rho_C^2} e^{-a/2\sqrt{2}\rho_C} + \frac{3A_C}{\rho_C^2} e^{-a/2\rho_C} + \frac{6A_A}{\rho_A(\rho_A+\rho_B)} e^{-r_{AB}/\rho_A} + \frac{6A_A}{\rho_A(\rho_A+\rho_C)} e^{-r_{AC}/\rho_A} + \frac{3A_B}{\rho_B(\rho_B+\rho_C)} e^{-r_{BC}/\rho_B}. \tag{7}$$

5. THE ATTRACTIVE INTERACTIONS

The Madelung constant has been evaluated for the perovskite structure[9]. For the case when A is a monovalent cation, B is a divalent cation and C is a monovalent anion, the value of α is 12.3775.

The van der Waals coefficients C and D can be calculated from the pair coefficients c_{12} and d_{12} as follows. Let $S_n(xyz)$ represent the sum of $1/r^n$ over a simple cubic lattice with origin at the fractional coordinates xyz (neglect the term at the origin for $S_n(000)$). Consider now an A^+ ion. The rest of the lattice surrounding it can be described as the sum of the following sub-lattices: (a) A simple cubic lattice of A^+ ions with origin at 000, the ion at the origin being left out; (b) A simple cubic lattice of B^{2+} ions with origin at $\frac{1}{2}\frac{1}{2}\frac{1}{2}$; (c) Three simple cubic lattices of C^- ions with origins respectively at $\frac{1}{2}\frac{1}{2}0$, $\frac{1}{2}0\frac{1}{2}$ and $0\frac{1}{2}\frac{1}{2}$. We can similarly describe the lattice as seen by a B^{2+} ion or a C^- ion. Then, the van der Waals coefficients per molecule can be written as

$$C = \frac{1}{2}[S_6(000)c_{AA} + S_6(000)c_{BB} + \{3S_6(000) + 6S_6(\tfrac{1}{2}\tfrac{1}{2}0)\}c_{CC} + 2S_6(\tfrac{1}{2}\tfrac{1}{2}\tfrac{1}{2})c_{AB} + 6S_6(\tfrac{1}{2}\tfrac{1}{2}0)c_{AC} + 6S_6(\tfrac{1}{2}00)c_{BC}] \tag{8}$$

$$D = \frac{1}{2}[S_8(000)d_{AA} + S_8(000)d_{BB} + \{3S_8(000) + 6S_8(\tfrac{1}{2}\tfrac{1}{2}0)\}d_{CC} + 2S_8(\tfrac{1}{2}\tfrac{1}{2}\tfrac{1}{2})d_{AB} + 6S_8(\tfrac{1}{2}\tfrac{1}{2}0)d_{AC} + 6S_8(\tfrac{1}{2}00)d_{BC}]. \tag{9}$$

The factor of $\frac{1}{2}$ arises as a correction for double counting.

The sums occuring in (8) and (9) could not be traced in the literature and so they were evaluated by direct summation. The values obtained are listed in Table 3.

For the pair interaction coefficients c_{12} and d_{12}, the following variational results[10, 11] were used

$$c_{12} = \frac{1}{2}\frac{e\hbar}{m^{1/2}} \frac{\alpha_1\alpha_2}{\left(\frac{\alpha_1}{N_1}\right)^{1/2} + \left(\frac{\alpha_2}{N_2}\right)^{1/2}} \tag{10}\dagger$$

$$d_{12} = \frac{27\hbar^2}{8m}\alpha_1\alpha_2 \frac{\left[\left(\frac{\alpha_1}{N_1}\right)^{1/2} + \left(\frac{\alpha_2}{N_2}\right)^{1/2}\right]^2}{\left[\frac{\alpha_1}{N_1} + \frac{20}{3}\left(\frac{\alpha_1\alpha_2}{N_1N_2}\right)^{1/2} + \frac{\alpha_2}{N_2}\right]} \tag{11}$$

where α_1 and α_2 are the polarizabilities of the two ions and N_1 and N_2 are the effective numbers of electrons in the two ions participating in the interaction. The values of α for the ions of interest to this paper were taken from Refs. [14, 15] while values of N were obtained from [16].

6. CALCULATIONS ON PEROVSKITE-LIKE CRYSTALS

Most crystals having the perovskite structure are oxides of the form ABO_3 where A and B are respectively divalent and tetravalent cations. Since we do not have the repulsion parameters of tetravalent ions, we are not yet in a position to deal with these crystals. Fortunately, there are many perovskite-like crystals of the form ABC_3 where A is a monovalent cation, B is a divalent cation and C is F^-, Cl^-, Br^- or H^-. Since we

Table 3. Lattice sums for the simple cubic lattice

x	y	z	$S_4(xyz)$	$S_6(xyz)$	$S_8(xyz)$
0	0	0	- 2.8373	8.40153	6.94576
$\frac{1}{2}$	0	0	- 0.09593	133.813	515.837
$\frac{1}{2}$	$\frac{1}{2}$	0	- 0.58252	35.7421	65.9615
$\frac{1}{2}$	$\frac{1}{2}$	$\frac{1}{2}$	- 0.80193	20.6430	25.7816

†Equation (10) has an extra factor of 1/3 compared to the result in [10]. This was found necessary in order to obtain reasonable agreement in the alkali halides between the variational values and the more accurate values of Mayer[12] and Hajj[13].

have the repulsion parameters of these ions, we can make all the necessary calculations.

The calculations were carried out as follows. The observed value of dW_L/da was calculated through the Hildebrand equation of state[17]

$$\frac{dW_L(a)}{da} = 3a^2\left(-P + \frac{T\beta}{K}\right) \tag{12}$$

where P is the pressure (0 in all cases here), T is the temperature, β is the thermal expansivity and K is the compressibility. The term $T\beta/K$ is a small thermodynamic correction and was calculated by means of the approximate formula (see the Appendix),

$$\frac{T\beta}{K} = 6.624 \times 10^{-16}\frac{nT}{a^3} \tag{13}$$

where n is the number of ions per molecule and C.G.S. units are used for all quantities. The equilibrium lattice spacing was then obtained by equating (6) and (12). At this value of the lattice spacing, the quantity d^2W_L/da^2 was calculated through eqn (7). Where an experimental value of the bulk modulus is available, the true value of d^2W_L/da^2 was calculated through the derivative of the Hildebrand equation viz.,

$$\frac{d^2W_L(a)}{da^2} = \frac{2}{a}\frac{dW_L(a)}{da} + \frac{9a}{K} \times \left[1 + \frac{T}{K}\left\{\left(\frac{\partial K}{\partial T}\right)_P + \frac{\beta}{K}\left(\frac{\partial K}{\partial P}\right)_T\right\}\right]. \tag{14}$$

In evaluating (14), the following approximate result (see the Appendix) was used.

$$\frac{T}{K}\left\{\left(\frac{\partial K}{\partial T}\right)_P + \frac{\beta}{K}\left(\frac{\partial K}{\partial P}\right)_T\right\} = -6.624 \times 10^{-16}\frac{nKT}{a^3}. \tag{15}$$

It should be noted that the approximations (13) and (15), though crude, are not likely to affect the final results to any appreciable extent since P is the important term in (12) and the quantity

$$\frac{T}{K}\left\{\left(\frac{\partial K}{\partial T}\right)_P + \frac{\beta}{K}\left(\frac{\partial K}{\partial P}\right)_T\right\}$$

is small compared to unity.

Table 4 gives the results obtained on all the perovskite-like crystals studied. The fit between the calculated

Table 4. Predicted values of a and $d^2W_L(a)/da^2$ for various crystals in the perovskite structure

Crystal (ABC_3)	a (Å) Measured	a (Å) Calculated	Difference(%)	r_{AB}(Å)	r_{BA}(Å)	r_{AC}(Å)	r_{CA}(Å)	r_{BC}(Å)	r_{CB}(Å)	$d^2W_L(A)/da^2$(10^5erg/cm^2) Measured	Calculated	Difference(%)
$AgZnF_3$	3.98	3.969	-0.280	1.806	1.632	1.299	1.507	1.067	0.918	-	2.642	-
$CsCaF_3$	4.522	4.575	1.169	2.272	1.630	1.842	1.393	1.267	1.021	-	2.054	-
$CsCdBr_3$	5.33	5.630	(5.623)	2.770	2.105	1.920	2.061	1.282	1.533	-	1.297	-
$CsCdCl_3$	5.20	5.328	2.465	2.622	1.992	1.897	1.871	1.272	1.392	-	1.503	-
$CsHgBr_3$	5.77	5.725	-0.784	3.299	1.668	1.940	2.108	1.395	1.467	-	1.662	-
$CsHgCl_3$	5.44	5.451	0.195	3.086	1.634	1.923	1.931	1.393	1.332	-	1.913	-
$CsPbBr_3$	5.874	5.942	1.156	2.772	2.374	1.985	2.216	1.491	1.480	-	1.180	-
$CsPbCl_3$	5.605	5.655	0.894	2.634	2.263	1.968	2.031	1.483	1.345	-	1.338	-
$CsPbF_3$	4.81	4.872	1.286	2.258	1.961	1.908	1.536	1.468	0.967	-	1.743	-
$KCaF_3$	4.371	4.418	1.077	2.063	1.764	1.567	1.557	1.247	0.962	-	1.995	-
$KCdF_3$	4.293	4.364	1.654	2.012	1.767	1.555	1.531	1.235	0.947	-	1.999	-
$KCoF_3$	4.069	3.987	-2.009	2.318	1.135	1.466	1.354	0.971	1.023	-	2.807	-
$KFeF_3$	4.122	4.007	-2.790	2.339	1.131	1.470	1.363	0.985	1.019	-	2.807	-
$KMgF_3$	3.973	3.997	0.613	2.216	1.245	1.468	1.358	0.985	1.014	2.591	2.698	4.14
$KMnF_3$	4.190	4.069	-2.877	2.331	1.193	1.485	1.392	1.026	1.008	2.434	2.727	12.06
$KNiF_3$	4.012	3.933	-1.970	2.319	1.087	1.453	1.328	0.931	1.035	-	2.868	-
$KZnF_3$	4.055	4.099	1.088	2.107	1.443	1.492	1.406	1.078	0.971	-	2.476	-
$LiBaF_3$	3.996	5.006	(25.28)	1.298	3.037	0.977	2.563	1.534	0.969	-	1.377	-
$LiBaH_3$	4.023	4.803	(19.39)	1.246	2.913	0.892	2.504	1.547	0.854	-	0.979	-
$LiEuH_3$	3.796	4.530	(19.34)	1.677	2.246	0.869	2.334	1.431	0.834	-	1.314	-
$LiSrH_3$	3.833	4.436	(15.73)	1.310	2.532	0.862	2.275	1.389	0.829	-	1.190	-
NH_4CoF_3	4.129	4.030	-2.392	2.319	1.172	1.525	1.325	0.973	1.042	-	2.909	-
NH_4MnF_3	4.241	4.103	-3.245	2.324	1.229	1.539	1.363	1.028	1.024	-	2.816	-
NH_4NiF_3	4.075	3.983	-2.263	2.326	1.123	1.516	1.300	0.933	1.058	-	2.979	-
$NaMgF_3$	3.955	3.859	-2.440	2.005	1.337	1.185	1.543	0.976	0.953	-	2.789	-
$RbCaF_3$	4.432	4.438	0.124	2.096	1.764	1.661	1.491	1.252	0.977	-	2.046	-
$RbCoF_3$	4.062	4.076	0.351	2.380	1.150	1.582	1.301	0.974	1.064	-	2.838	-
$RbFeF_3$	4.174	4.092	-1.966	2.400	1.144	1.585	1.308	0.988	1.058	-	2.835	-
$RbMgF_3$	4.095	4.087	-0.201	2.276	1.264	1.584	1.306	0.990	1.053	-	2.745	-
$RbMnF_3$	4.250	4.144	-2.485	2.383	1.206	1.596	1.335	1.029	1.043	-	2.757	-
$TlCoF_3$	4.138	4.040	-2.364	2.372	1.127	1.587	1.269	0.973	1.047	-	2.883	-
root mean square error			1.803									9.02
Mean absolute error			1.544									9.10

values of the lattice spacings and the experimental values[16, 17] is reasonably good, the r.m.s. error being 1.80%. Experimental values of compressibility are listed by Hearman[8] for only two crystals viz., $KMnF_3$ and $KMgF_3$. For these two cases, there is excellent agreement between the measured and calculated values of d^2W_L/da^2. This is a gratifying result when we consider the fact that all the repulsion parameters used in this study were refined in simpler systems and have been transferred *unaltered* to the present complex system.

Table 4 lists the "radii" of the various ions in the direction of their various neighbours. A study of these emphasizes the asymmetric compression of the ions which is a basic characteristic of the present theory[4]. The halogen ions, e.g. are very much more compressed in the direction of their B neighbours than in the direction of their A neighbours. Moreover, the "radius" of Br^- in the direction of the Pb^{2+} neighbours in $CsPbBr_3$ is 1.480 Å and the corresponding "radius" of Cl^- in $CsPbCl_3$ is 1.345 Å, whereas the average "radius" of Br^- in the alkali halides is about 1.90 Å and that of Cl^- is about 1.75 Å[5]. It should be remembered that the respulsion parameters of Br^- and Cl^- were determined entirely from the data on the alkali halides where they exist with these larger "radii". *Our ability to use the same parameters even when the ions are in such compressed states as in the crystals considered here indicates that the parameters we have refined have a wide range of validity.* This is rather heartening.

Another point to be noted is that we have studied compounds containing such ions as Ag^+ and Hg^{2+} which do not seem to fit in very well with the present ionic approach (Section 2). In spite of this fact, we find that the repulsion parameters that were obtained earlier for these ions are quite successful when applied to the perovskite-type crystals $AgZnF_3$, $CsHgBr_3$ and $CsHgCl_3$. A possible explanation is that the sizes of these ions are predicted reasonably well, however unreliable their repulsion parameters may be, and so the lattice spacings of the corresponding perovskite-type crystals are in reasonable agreement with the experimental values. As a corollary, we feel that the values of d^2W_L/da^2 predicted for these crystals are not reliable.

†A fifth crystal viz., $CsCdBr_3$, also shows a discrepancy which, however, we are unable to explain. The experimental situation may bear further investigation.

7. CALCULATIONS ON INVERSE PEROVSKITE STRUCTURE CRYSTALS

Table 4 shows that the calculated values of the lattice spacings of $LiBaF_3$, $LiBaH_3$, $LiEuH_3$ and $LiSrH_3$ do not agree with experiment,† being 15–25% too high. It was therefore suspected that these crystals may be of the inverse perovskite structure, i.e. with the divalent ions at the cube corners (Fig. 1). The necessary theory for such a structure is easily developed and eqns (1), (6) and (7) can be used, provided A and B are systematically interchanged.

The Madelung constant for the inverse perovskite structure could not be located in the literature. It was evaluated to be 10.9177 by methods similar to those described in Section 5. The relevant lattice sums $S_1(xyz)$ have been discussed by Naor[20] and are listed in Table 3. The van der Waals coefficients can be calculated by relations similar to (8) and (9).

The results obtained on $LiBaF_3$, $LiBaH_3$, $LiEuH_3$ and $LiSrH_3$, assuming them to be of the inverse perovskite structure, are shown in Table 5. The fit in lattice spacing is seen to be much improved over that obtained in Table 4, strongly supporting the idea that these four crystals are indeed inverse perovskite types.

The lattice energies in the two structure types were calculated using eqn (1). For instance, for $LiBaF_3$, the energy turned out to be −720.7 Kcal/mole in the perovskite structure and −789.3 Kcal/mole in the inverse perovskite structure, suggesting that this crystal is more stable in the inverse perovskite form. It is satisfying that, using our theory, both the lattice spacing calculation and the energy calculation strongly support the hypothesis that $LiBaF_3$ prefers the inverse perovskite structure.

The relative stability of the perovskite and inverse perovskite forms cannot be predicted on the basis of packing alone. This is because the electrostatic interaction is much stronger in the former, as can be seen by its higher value of α. Thus, a more loosely packed perovskite structure could be more stable than a more tightly packed inverse perovskite structure. Table 6 compares the predicted lattice spacings and binding energies of all the crystals in both the perovskite and inverse perovskite structures. The crystal $NaMgF_3$ is of particular interest here. We notice that the theory predicts a smaller value of the lattice spacing and hence a more compact packing for this crystal in the inverse perovskite structure. Still, its binding energy is only −803.8 Kcal/mole in the

Table 5. Predicated values of a and $d^2W_L(a)/da^2$ for some crystals in the inverse perovskite structure

Crystal (ABC_3)	Measured a (Å)	Calculated a (Å)	Difference (Å)	r_{AB} (Å)	r_{BA} (Å)	r_{AC} (Å)	r_{CA} (Å)	r_{BC} (Å)	r_{CB} (Å)	$\frac{d^2W_L}{da}$ (10^5 erg/cm^2)
$LiBaF_3$	3.996	4.055	1.485	1.055	2.457	0.732	1.296	1.649	1.218	2.477
$LiBaH_3$	4.023	4.146	3.049	1.078	2.512	0.738	1.335	1.674	1.257	1.499
$LiEuH_3$	3.796	3.889	2.459	1.370	1.998	0.723	1.222	1.478	1.272	1.302
$LiSrH_3$	3.833	3.918	2.207	1.149	2.244	0.724	1.235	1.494	1.276	1.636
Root mean square error			2.367							
Mean absolute error			2.300							

Table 6. Predicted lattice spacings and binding energies of various crystals in the perovskite and inverse perovskite structures

Crystal	Measured a (Å)	Calculated a (Å)				Binding energy (Kcal/mole)	
		Perovskite	Difference (%)	Inverse perovskite	Difference (%)	Perovskite	Inverse perovskite
$AgZnF_3$	3.98	3.969	-0.280	4.133	3.839	-904.8	-769.3
$CsCaF_3$	4.522	4.575	1.169	5.390	19.20	-798.2	-597.4
$CsCdBr_3$	5.33	5.630	5.623	6.516	22.25	-664.0	-506.5
$CsCdCl_3$	5.20	5.328	2.465	6.223	19.67	-699.7	-529.7
$CsHgBr_3$	5.77	5.725	-0.784	6.480	12.31	-677.7	-510.4
$CsHgCl_3$	5.44	5.451	0.195	6.188	14.75	-710.3	-532.7
$CsPbBr_3$	5.374	5.942	1.156	6.496	10.60	-636.3	-509.5
$CsPbCl_3$	5.605	5.655	0.894	6.205	10.70	-666.2	-531.7
$CsPbF_3$	4.81	4.372	1.296	5.373	11.71	-754.4	-601.0
$KCaF_3$	4.371	4.418	1.077	4.520	3.411	-815.3	-639.8
$KCdF_3$	4.293	4.364	1.654	4.510	5.060	-823.3	-695.5
$KCoF_3$	4.069	3.987	-2.009	4.474	9.959	-905.1	-696.3
$KFeF_3$	4.122	4.007	-2.790	4.474	8.549	-902.0	-696.3
$KMgF_3$	3.973	3.997	0.613	4.476	12.66	-900.3	-696.3
$KMnF_3$	4.190	4.069	-2.877	4.477	6.860	-889.9	-696.1
$KNiF_3$	4.012	3.933	-1.970	4.472	11.47	-915.6	-696.4
$KZnF_3$	4.055	4.099	1.088	4.477	10.40	-878.9	-697.4
$LiBaF_3$	3.996	5.006	25.28	4.055	1.485	-720.7	-789.3
$LiBaH_3$	4.023	4.803	19.39	4.146	3.049	-707.5	-728.9
$LiEuH_3$	3.796	4.530	19.34	3.889	2.459	-761.1	-771.7
$LiSrH_3$	3.833	4.436	15.73	3.918	2.207	-760.8	-761.5
NH_4CoF_3	4.129	4.030	-2.392	4.772	15.55	-901.2	-668.4
NH_4MnF_3	4.241	4.103	-3.245	4.773	12.55	-887.2	-668.3
NH_4NiF_3	4.075	3.983	-2.263	4.771	17.09	-910.7	-668.4
$NaMgF_3$	3.955	3.859	-2.440	3.819	-3.443	-924.7	-803.8
$RbCaF_3$	4.452	4.458	0.124	4.904	10.15	-812.4	-651.6
$RbCoF_3$	4.062	4.076	0.351	4.890	20.38	-892.4	-651.6
$RbFeF_3$	4.174	4.092	-1.966	4.890	17.16	-889.9	-651.6
$RbMgF_3$	4.095	4.087	-0.201	4.890	19.43	-888.1	-651.7
$RbMnF_3$	4.250	4.144	-2.485	4.891	15.09	-879.7	-651.6
$TlCoF_3$	4.138	4.040	-2.364	4.789	15.73	-901.8	-662.7

inverse perovskite structure whereas it is −924.7 Kcal/mole in the perovskite structure. On the other hand, in $LiSrH_3$, the lattice spacing in the inverse perovskite structure is substantially smaller than in the perovskite structure, but the two binding energies are nearly equal. On the basis of our theory, we can say that for $LiSrH_3$ the inverse perovskite structure is only marginally more stable. The possibility of making such comparisons and predictions greatly enhances the value of the present theory. Table 6 shows that in all cases, the calculated binding energies correctly predict the experimentally observed structure to be energetically the more stable one.

Among the four inverse perovskite crystals listed in Table 4, $LiBaF_3$ has been experimentally shown[21] to be inverse perovskite. This has been done by measuring the intensities of its X-ray powder lines and comparing them with the values expected for the two structures. In fact, we became aware of this work only after we had already concluded from our calculations that $LiBaF_3$ should be inverse perovskite. In the other three cases, viz., $LiBaH_3$, $LiEuH_3$ and $LiSrH_3$, the respective authors[22, 23] only *conjecture* that the inverse perovskite structure is likely. The X-ray powder patterns cannot resolve the ambiguity because the scattering factors of Li^+ and H^- are nearly identical and negligibly small compared to that of the divalent cations. The present calculations summarized in Table 6 clearly indicate that these crystals should be of the inverse perovskite structure. In the case of $LiSrH_3$ alone the binding energies in the two structures are nearly equal and we are unable to predict the structure unequivocally. However, the calculated lattice spacings resolve the ambiguity. Neutron diffraction experiments would be able to identify the structures of all these crystals and it would be interesting to see how well they agree with our theoretical predictions.

The fact that the calculated binding energies of $LiSrH_3$

in the two structures are so close together implies that this crystal may transform under the action of temperature or pressure. Calculations are under way to approximately predict the conditions under which such a transformation is likely to occur. Experiments along these lines would be quite interesting.

Acknowledgement—The authors wish to thank Rajaram Nityananda for helpful discussions.

REFERENCES

1. Tosi M. P., *Solid State Physics* (Edited by F. Seitz and D. Turnbull), Vol. 16, p. 1. Academic Press, New York (1964).
2. Narayan R. and Ramaseshan S., *Pramana* **3**, 143 (1974).
3. Narayan R. and Ramaseshan S., *J. Phys. Chem. Solids* **37**, 395 (1976).
4. Ramaseshan S. and Narayan R., *Curr. Sci.* **45**, 357 (1976).
5. Narayan R. and Ramaseshan S., *Curr. Sci.* **46**, 359 (1977).
6. Bridgman P. W., *Proc. Am. Acad. Arts Sci.* **74**, 21 (1940).
7. Bridgman P. W., *Proc. Am. Acad. Arts Sci.* **76**, 9 (1945).
8. Hearman R. F. S., Landolt-Börnstein, *Numerical Data and Functional Relationships in Science and Technology*, Vol. III/2, p. 1. Springer-Verlag, Berlin (1969).
9. Johnson Q. C. and Templeton D. H., *J. Chem. Phys.* **34**, 2004 (1961).
10. Margenau H., *Rev. Mod. Phys.* **11**, 1 (1939).
11. Narayan R., *J. Phys. Chem. Solids* **38**, 1097 (1977).
12. Mayer J. E., *J. Chem. Phys.* **1**, 270 (1933).
13. Hajj F., *J. Chem. Phys.* **44**, 4618 (1966).
14. Tessman J., Kahn A. and Shockley W., *Phys. Rev.* **92**, 890 (1953).
15. Pauling L., *Proc. R. Soc.* **A114**, 191 (1927).
16. Scott R. A. and Scheraga H. A., *J. Chem. Phys.* **42**, 2209 (1965).
17. Hildebrand J. H., *Z. Physik* **67**, 127 (1931).
18. Wyckoff R. W. G., *Crystal Structures*. Interscience, New York (1971).
19. Galasso F. S., *Structure, Properties and Preparations of Perovskite-type compounds*. Pergamon, Oxford (1969).
20. Naor P., *Z. Krist.* **110**, 112 (1958).
21. Ludekens W. L. W. and Welch A. J. E., *Acta Cryst* **5**, 841 (1952).
22. Messer C. E., Eastman J. C., Mers R. G. and Maeland A. J., *Inorg. Chem.* **3**, 776 (1964).
23. Messer C. E. and Hardcastle K., *Inorg. Chem.* **3**, 1327 (1964).

APPENDIX

Some thermodynamic approximations

Consider the Gruneisen's constant γ

$$\gamma = \frac{V\beta}{C_V K} \tag{A1}$$

where V is the volume per molecule, β is the thermal expansivity, C_v is the specific heat per molecule at constant volume and K is the compressibility. It is experimentally known that γ is almost constant over a wide range of temperature. We assume here that γ is independent of pressure and that all crystals have the same value of γ which is taken to be 1.6 based on the data available for the alkali halides. We also assume that C_v is equal to the classical value

$$C_V = 3nk \tag{A2}$$

where n is the number of ions per molecule and k is the Boltzmann constant. Equation (A1) then leads to

$$\frac{\beta}{K} = 6.624 \times 10^{-16} \frac{n}{a^3} \tag{A3}$$

where a^3 is V, the volume per molecule and all quantities are measured in C.G.S. units.

Further we know from thermodynamics that

$$\left(\frac{\partial K}{\partial T}\right)_P = -\left(\frac{\partial \beta}{\partial P}\right)_T \tag{A4}$$

Using (A1) we see that

$$\left(\frac{\partial \beta}{\partial P}\right)_T = \frac{\beta}{K}\left(\frac{\partial K}{\partial P}\right)_T - \beta K. \tag{A5}$$

Thus we obtain the result that

$$\frac{T}{K}\left\{\left(\frac{\partial K}{\partial T}\right)_P - \frac{\beta}{K}\left(\frac{\partial K}{\partial P}\right)_T\right\} = -\beta T = -6.624 \times 10^{-16} \frac{nKT}{a^3}. \tag{A6}$$